IFSCC 2025 full paper (IFSCC2025-1230)

Preparation and Study of Novel GHK-Cu-Loaded Ginsenoside Liposomes for Anti-Aging Activity

Fei Shi [1], Shaohua Ren [2*], Fang Lin [1], Yaqi Wang [1], Feifei Wang [3,4], Wenrou Su [3,4], Yuqi Zhao [3,4], Yongshi Chen [2], Xue Li [2], Yukun Gu [2], Jihua Liu [1*]

[1] School of Pharmaceutical Sciences, Jilin University, Changchun, China; [2] cBioMey (Guangzhou) Technology Co., Ltd., Guangzhou, China; [3] Yunnan Botanee Bio-technology Group Co., Ltd., Yunnan, China; [4] Yunnan Characteristic Plant Extraction Laboratory, Yunnan Characteristic Plant Extraction Laboratory Co., Ltd., Yunnan, China

*: Correspondence:
Jihua Liu, email: liujh@jlu.edu.cn; Shaohua Ren, email: renshaohua@cbiomey.com

Abstract

Copper Tripeptide-1 (GHK-Cu) is a powerful cosmetic ingredient, known for stimulating collagen synthesis, reversing aging, promoting skin healing, and reducing scarring. However, its highly hydrophilic nature makes it hard to penetrate the stratum corneum of the skin. To address this challenge, we encapsulated GHK-Cu in an innovative nanoliposome with ginsenosides (GS) for enhancing transdermal absorption and anti-aging effectiveness. Additionally, ginsenoside plays an active role and acts as an excipient in its preparation. We investigated the conformation, polarity, and energy transfer mechanisms of the GHK-Cu-GS complex using fluorescence spectroscopy, and UPLC/QTOF-MS. Our findings reveal that the interaction between GHK-Cu and GS significantly formed a novel complex and enhances the stability of liposomes. Notably, the addition of GS resulted in superior encapsulation efficiency. This enhancement maybe attributed to the supramolecular interaction of GS and GHK-Cu. Ginsenoside can serve as a stable "shell" layer for nanocarriers, facilitating the effective encapsulation. Overall, the combination of ginsenoside and GHK-Cu offers a promising new strategy against skin aging.

Keywords GHK-Cu, ginsenoside, supramolecular complex, novel co-liposomes

---

1. Introduction

Copper Tripeptide-1 (GHK-Cu) is a powerful cosmetic ingredient, known for stimulating collagen synthesis, reversing aging, promoting skin healing, and reducing scarring [1-3]. However, its highly hydrophilic nature makes it hard to penetrate the stratum corneum of the skin [4]. Ginsenosides (GS), the primary bioactive components of Panax Ginseng, exhibit antitumor, anti-aging, antioxidant, and anti-apoptotic properties [5–7]. It was reported that novel nano-co-delivery liposomes constructed with ginsenosides not only improve liposomal stability

and prolong circulation time, but also exhibit active targeting capabilities and synergistic interactions with co-loaded drugs [8,9]. In this study, we developed a novel nano-liposomal system incorporating ginsenosides to encapsulate GHK-Cu (GHK-Cu@GS-LP), aiming to enhance its skin permeability and amplify its anti-aging effects. Multiple spectroscopic analyses [10] confirmed the formation of a supramolecular complex between ginsenosides and GHK-Cu. This interaction improved the stability and functionality of the nano-liposomes, representing an innovative preparation method. The application of this novel nano-liposomal system in anti-aging skincare products holds significant potential to advance the cosmetics industry.

There are various factors that contribute to skin aging, and the anti-aging benefits of any single active are limited. Ginsenoside liposomes have the ability to encapsulate both water-soluble ingredients and insoluble active ingredients. Additionally, we have developed co-delivered ginsenoside liposomes that encapsulate both Palmitoyl Hexapeptide-12 (an insoluble ingredient) and Nonapeptide-1 (a water-soluble ingredient) to enhance their firming and anti-aging effects on the skin.

2. Materials and Methods

2.1 Instruments

Liquid Chromatography-Mass Spectrometry; RF-6000 Fluorescence Spectrophotometer; FA1004B Analytical Balance; SCILOGEX MX-F Adjustable Vortex Mixer; Rotary evaporator; Ultraviolet-visible (UV-Vis) microvolume spectrophotometer; PCR thermal cycler.

2.2 Materials and Reagents

Egg yolk lecithin; Ginsenoside (made in our lab); Copper Tripeptide-1; Sodium Deoxycholate; Acetonitrile; Trifluoroacetic acid; Palmitoyl Hexapeptide-12; Nonapeptide-1; Human adult dermal fibroblasts (HDFa cells); cDNA synthesis kit; ELISA kit PC-1 (type I procollagen).

2.3 Preparation and characterization of liposomes

We developed a novel nano-liposomal system incorporating ginsenosides to encapsulate GHK-Cu (GHK-Cu@GS-LP) by thin film dispersion method. Similarly, we prepared blank liposomes (LP) and GHK-Cu-loaded liposomes with cholesterol (GHK-Cu@LP) for comparison. The morphology of liposomes was also observed by transmission electron microscopy (TEM). Under the condition of 25 ± 0.1 ℃, take an appropriate amount of liposome solution diluted with distilled water, and measure the particle size, Zeta potential, and PDI using a Malvern laser particle size analyzer. Encapsulation rate detection was detected by high-performance liquid chromatography.

2.4 Preparation of sample solution in fluorescence experiment

GHK-Cu solution was 1mg/mL in ultra-pure water, GS solution was also 1mg/mL in ultra-pure water. They were mixed to varying concentrations of GHK-Cu and GS (0.25 mg/mL GHK-Cu + 0.025mg/mL to 0.50 mg/mL GS).

2.5 Fourier Transform Infrared Spectroscopy Detection (FTIR)

The GHK-Cu, GS and GHK-Cu -GS freeze-dried powders were mixed with potassium bromide as a ratio of 1:50 in a mold to test using a Fourier Transform Infrared Spectrometer, respectively. The infrared spectrum was determined in the resolution of 4 cm^{-1}, scanning speed of 5 times/s, and wavelength range of 400~4000 cm^{-1}.

2.6 Fluorescence emission spectroscopy detection

Samples were detected on a RF-6000 Fluorescence Spectrophotometer with excitation 280 nm, Emission 300-500 nm, 1.0 nm intervals, 298 K.

2.7 Fluorescence emission spectroscopy detection at different temperatures

The samples were incubated at 27 ℃ (300.15K), 37 ℃ (310.15K), and 47 ℃ (320.15K) for 15 minutes, then detected on a fluorescence spectrophotometer with 275 nm excitation, 295-530 nm emission, and 1.0 nm intervals.

2.8 Resonance light scattering spectrum (RLS) of GS interacting with GHK-Cu

Samples were performed resonance light scattering detection using a fluorescence spectrophotometer with 275 nm excitation, 275-500 nm emission, and 1.0 nm intervals.

2.9 Fluorescence emission spectrum detection at different temperatures

Three sets of sample solutions (prepared as the description under item 2.4 were prepared in parallel and subjected to a constant temperature water bath at 27°C (300.15K), 37°C (310.15K), and 47°C (320.15K) for 15 minutes, and analyzed using the RF-6000 fluorescence spectrophotometer with 240 nm excitation, 260-460 nm emission, 1.0 nm intervals.

2.10 LC-QTOF-MS Detection of the Binding Constant of GHK-Cu combined with GS

Sample solutions containing 3 mg/mL GHK-Cu and 0, 3.0, 3.6, 4.8, 5.4, 6.0 mg/mL GS, respectively, were determined by the method of UPLC-QTOF-MS, with BEH C18 column, acetonitrile-water (0.1% formic acid, 0.4 mL/min), MS conditions of ESI source, negative ion mode, MS^E Continum, scan range 50-2000 Da, and collision energy 6-20 V. According to the formula derived by Loukas, the binding constant (K_{st}) is calculated by plotting a scatchard-style plot based on the ratio of the ion counts of the guest molecule (GHK-Cu) to the complex ($1/\Delta I_r$) against the concentration of the host ($1/C_H$). The ratio of the intercept to the slope of this linear plot gives the binding constant (K_{st}). The formula and derivation process are as follows:

$$\frac{1}{\Delta I_r} = \frac{1}{K_{st}K_C C_H C_G} + \frac{1}{C_G K_C} \quad \Leftrightarrow \quad \frac{1}{\Delta I_r} = \frac{1}{K_{st}K_C C_G} \times \frac{1}{C_H} + \frac{1}{C_G K_C}$$

(Plot $1/\Delta I_r$ against $1/C_H$, where the ratio of intercept to slope is K_{st})

$$I_0 \approx 0 \quad \Delta I_r = I_r - I_0 \approx I_r \quad I_r = \frac{I_{HG}}{I_{HG}+I_G}$$

Among them, K_C is the proportionality constant, K_{st} is the binding constant, C_H is the initial concentration of the host, C_G is the initial concentration of the guest, I_{HG} is the count of complex ions, I_G is the count of guest ions, I_r is the ionization efficiency, and I_0 is the initial ionization efficiency.

2.11 Evaluation of the efficacy of co-delivered ginsenoside liposomes containing Palmitoyl Hexapeptide-12 and Nonapeptide-1 (Duotide Pro)

Testing of Duotide Pro in zebrafish models for anti-wrinkle and firming effects

The zebrafishes were divided into two groups, a normal control group and a sample group (the samples were ingested into the zebrafishes by dissolving them into water for fish farming). After absorbing the samples for 24 hours, the transcript levels of the skin collagen col1a1a, col1a1b, eln1, and eln2 genes were detected by qPCR, and their relative expression were calculated.

Testing of Duotide Pro in fibroblast for anti-Aging effects

Human adult dermal fibroblasts (HDFa cells) were treated with 200 μM hydrogen peroxide (H_2O_2) for 2 hours, followed by the addition of the test compound and subsequent incubation for 48 hours. Cell culture supernatants were then collected, and human procollagen type I (PC-1) secretion levels were quantified using a commercially available ELISA kit.

3. Results

3.1 Morphology assay

The hydrated liposomes are uniform and semi-transparent liquid, and there is no layering or precipitation observed at room temperature, indicating good appearance (Figure 1). The

results of TEM were shown in Figure 2. LP did not appear spherical or spherical like, with irregular distribution. GHK-Cu@GS-LP appeared spherical with no obvious rupture or adhesion, and the size was uniform.

Figure 1. Different GHK-Cu liposome morphology (from right to left, GHK-Cu@GS-LP, GHK-Cu@LP, GHK-Cu)

3.2 Particle size, PDI, and Zeta potential assay

As shown in Table 1 and Figure 2, the GHK-Cu@GS-LP size is 99.76 ± 1.27 nm, and due to the interaction between total ginsenosides and GHK Cu, liposomes become more concentrated and stable. GHK-Cu@LP size is 133.60 ± 1.51 nm, which is larger than GHK-Cu@GS-LP because of the presence of cholesterol. The Zeta potential is -40.13 ± 1.03 mV, indicating that GHK-Cu@GS-LP had high stability, with a PDI of 0.12 ± 0.04, proving that GHK-Cu@GS-LP have a good particle size distribution.

Table 1. Characterization of GHK-Cu@GS-LP and GHK-Cu@LP

	Size (nm)	PDI	Zeta Potential (mV)	EE (%)
GHK-Cu@GS-LP	99.76 ± 1.27	0.12 ± 0.04	-40.13 ± 1.03	79
GHK-Cu @ LP	133.60 ± 1.51	0.19 ± 0.02	-31.43 ± 0.79	64

3.3 Detection results of encapsulation efficiency

The encapsulation efficiency (EE) of GHK-Cu@LP is 64%, the encapsulation efficiency of GHK-Cu@GS-LP was increased to 79%. The results showed that ginsenosides significantly improved the encapsulation efficiency of GHK-Cu in liposomes.

3.4 The complex formation of GHK-Cu and GS characterized by multi-spectroscopic methods

The FTIR spectrum showed GHK-Cu-GS complex formation with the peak of C=O changed from 1571 to 1578 cm^{-1}, and the peak of -OH changed from 3388 to 3394 cm^{-1}, comparing with GHK-Cu, and there was no peak of C=O showed in GS spectrum (Figure 3 a).

The results of fluorescence emission spectroscopy indicated that the maximum emission wavelength has shifted from 305nm to 308nm, indicating a change in the microenvironment of GHK Cu in the complex and an interaction between GHK Cu and GS (Figure 3 b).

The results of RLS indicated that the fluorescence intensity gradually increased as the concentration of GS increased, indicating the formation of the complex (Figure 3 c).

In temperature-dependent fluorescence experiment, it was showed that GHK-Cu-GS complex formed with a large binding constant, and temperature has a small effect on it, indicating a strong binding between them (Table 2). According to Table 3, $\Delta G<0$ indicates that the reaction proceed spontaneously; $\Delta H<0$ indicates that the reaction is an exothermic process; $\Delta S>0$ and $\Delta H<0$ indicate that the interaction in complex between GHK-Cu and GS is mainly hydrophobic and hydrogen bonding (Figure 3 d and e).

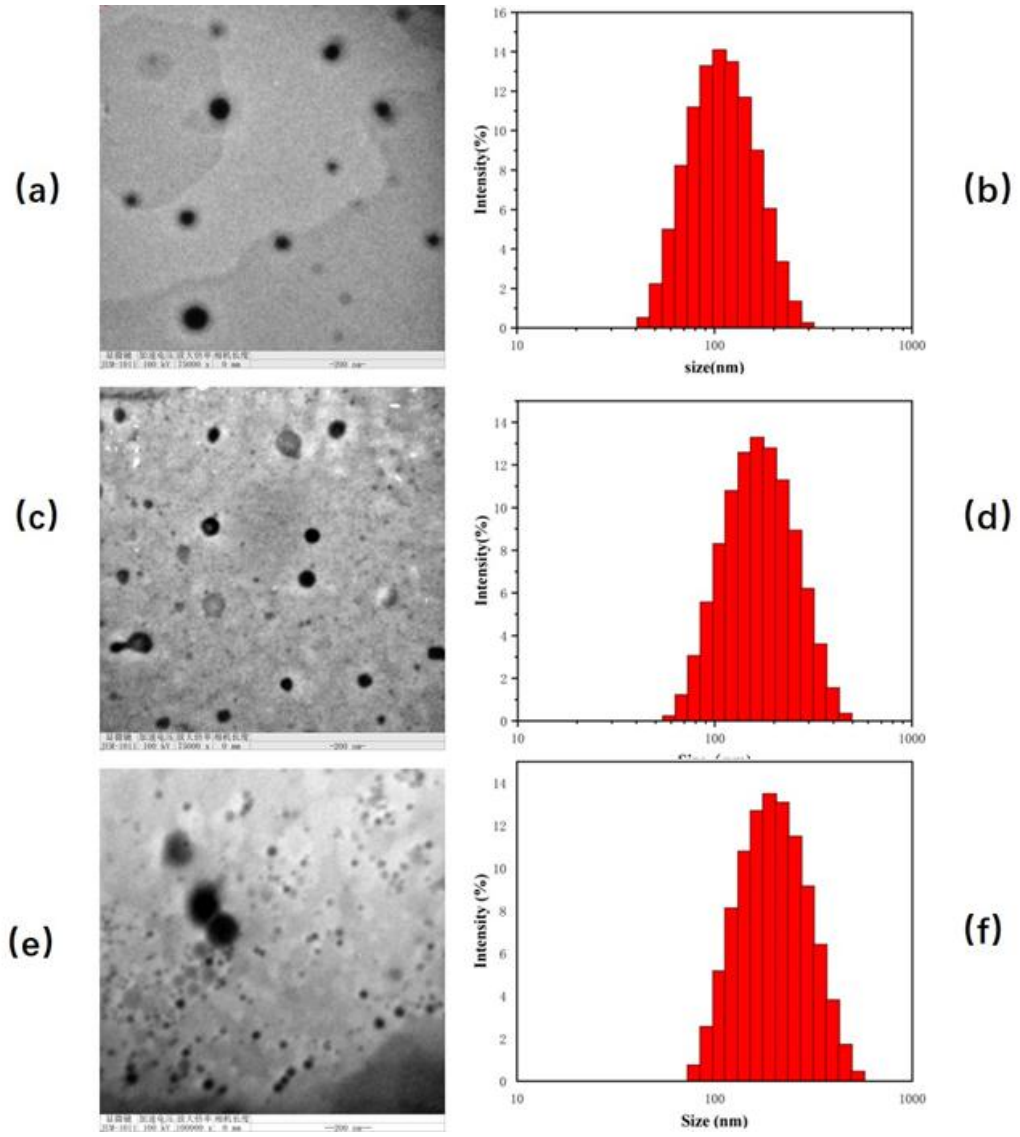

Figure 2. Characterization of lipid body with TEM and particle size. (a) TEM of GHK-Cu@GS-LP; (b) TEM of GHK-Cu@LP; (c) TEM of LP; (d) hydration size of GHK-Cu@GS-LP; (e) hydration size of GHK-Cu@LP; (f) hydration size of LP

Table 2. Binding constants of GHK-Cu and GS in temperature-dependent fluorescence experiment

T/K	Ka (L/g)	R^2
300.15	5.81×10^4	0.991
310.15	5.33×10^4	0.997
320.15	4.82×10^4	0.993

Table 3. Thermodynamic parameters of GS and GHK-Cu reaction in temperature-dependent fluorescence experiment

T/K	$\Delta H^\ominus$ (kJ mol^{-1})	$\Delta S^\ominus$ (Jmol^{-1} K^{-1})	$\Delta G^\ominus$ (kJ mol^{-1})
300.15	-	-	-27.38
310.15	-7.58	65.96	-28.04
320.15	-	-	-28.70

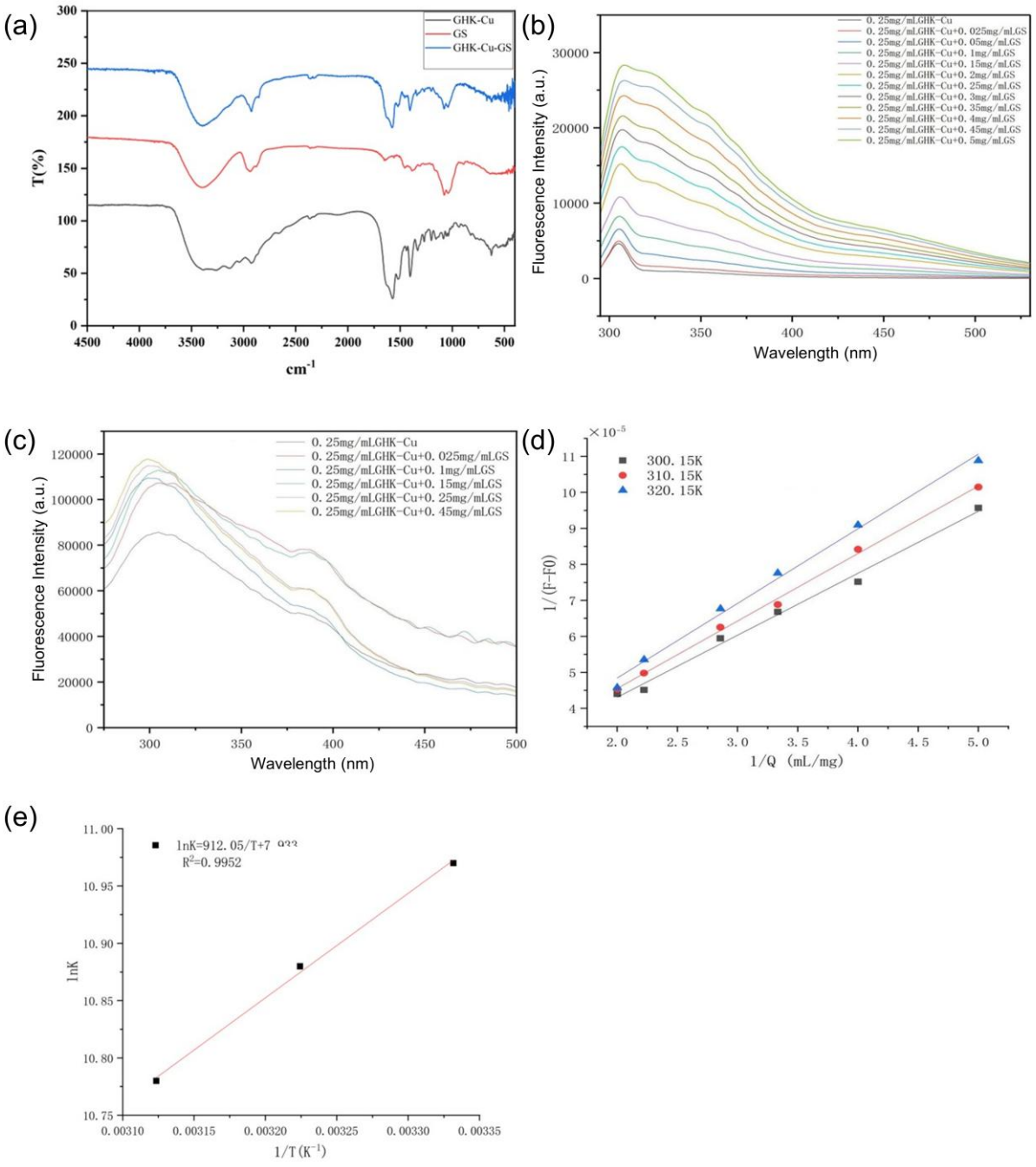

Figure 3. Characterization of complex GHK-Cu-GS by multi-spectroscopic methods. (a) FTIR spectrum of GHK-Cu, GS and GHK-Cu-GS; (b) Fluorescence spectra of GHK-Cu under the influence of different concentrations of GS; (c) RLS spectra of GSH and different concentrations of GS. (d) The Stern-Volmer plot of GHK-Cu at different temperatures. (e) The Van't Hoff curve of GHK-Cu

3.5 The Binding Constant of GHK-Cu and GS determined by UPLC-QTOF-MS Method

UPLC-QTOF-MS coupled with UNIFI platform was used to identify the complex of GHK-Cu-GS. Based on information such as total ion chromatogram, mass spectrometry, retention time, and response value, component screening was performed. Combined with literature and mass spectrometry fragmentation rules, the complexes of GHK-Cu and two ginsenosides, Rg1 and

Rg2 were finally identified from the sample. The identification results are shown in Table 4 and Figure 4.

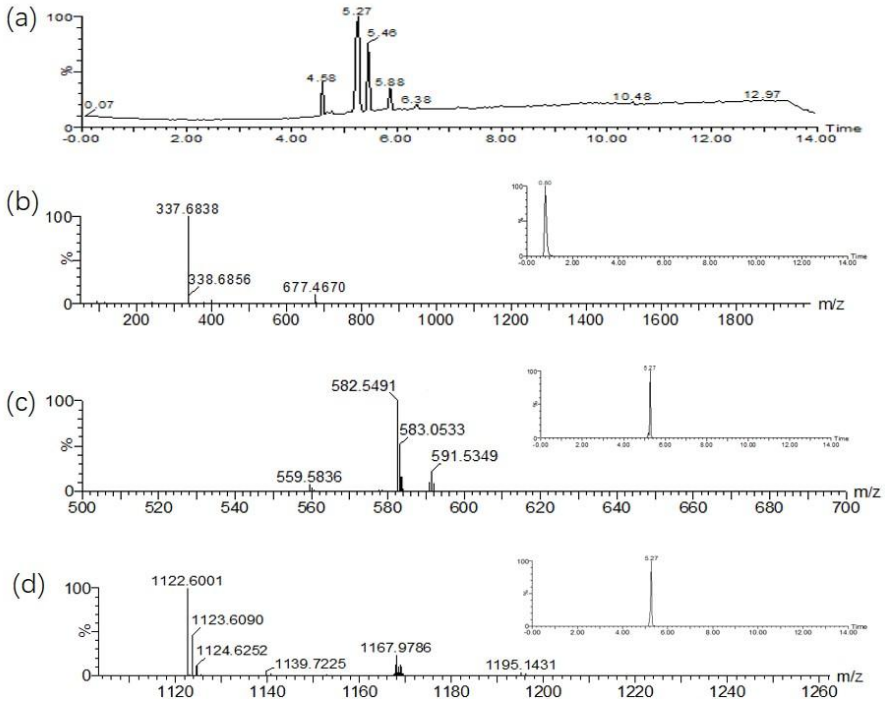

Figure 4. MS spectrum and ion chromatogram of the complex GHK-Cu-Rg1 and GHK-Cu-Rg2. (a) Total ion chromatogram in negative ion mode; (b) MS spectrum and extracted ion chromatogram of GHK-Cu; (c) Mass spectrum and extracted ion chromatogram of GHK-Cu-Rg1;(d) Mass spectrum and extracted ion chromatogram of GHK-Cu-Rg2

Table 4. The complexes of GHK-Cu-Rg1 and GHK-Cu-Rg2 identified by UPLC-QTOF-MS

No.	RT/min	Formula	Neutral mass (Da)	Component name	Fragment ion (m/z)
1	5.27	$C_{56}H_{94}N_6O_{18}$	591.5349	GHK-Cu-Rg1	591.5349[M-Cu+HCOO]$^{3-}$ 582.5491[M-Cu+HCOO-H_2O]$^{3-}$ 568.6498[M-Cu-H]$^{3-}$
2	5.27	$C_{56}H_{94}N_6O_{17}$	1167.9788	GHK-Cu-Rg2	1167.9788[M-Cu+HCOO]$^{3-}$ 1166.9641[M-Cu+HCOO-H]$^{4-}$
3	0.80	$C_{14}H_{22}N_6O_4$	337.6838	GHK-Cu	337.6838[M-Cu-H]$^{3-}$ 、 400.6615[M-H]$^{-}$

3.6 Calculation of Binding Constants

GHK-Cu-Rg1 binding constant was calculated according on the slope and intercept of the straight line. The linear equation y=0.0077x+0.2364 was obtained, R^2 = 0.9909, and K_{st} was calculated as 30.70 (mol/L) $^{-1}$. GHK-Cu-Rg2 binding constant was 45.51 (mol/L) $^{-1}$, and the linear equation y=0.0451x-2.0527 is obtained, R^2 =0.9979.

3.7 Evaluation of the efficacy of Duotide Pro

We conducted a thorough evaluation of the encapsulation efficiency of Palmitoyl Hexapeptide-12 in Duotide Pro, both initially and after six months of storage. Remarkably, both

measurements were approximately 98% (Table 5). This outstanding result demonstrates the exceptional stability of Duotide Pro, highlighting its reliability and efficacy over time.

By testing the relative expression of anti-wrinkle related genes (col1a1a and col1a1b genes), we can know the Duotide Pro can significantly promote collagen col1a1a and col1a1b genes, indicating that it has anti-wrinkle effect (Figure 5 a and b). The relative expression of eln1 and eln2 genes can be tested to indicate whether the test substance has firming effects. Duotide Pro can significantly promote the expression of skin elastin eln1 and eln2 on the skin, suggesting a certain firming effect (Figure 5 c and d). A model of oxidative stress injury in HDFa cells was established using H_2O_2 stimulation to assess the firming and anti-aging effects of the test substance. Duotide Pro demonstrated a significant up-regulation of PC-1, outperforming the positive control group (VC+VE) and confirming its firming and anti-aging properties (Figure 5 e).

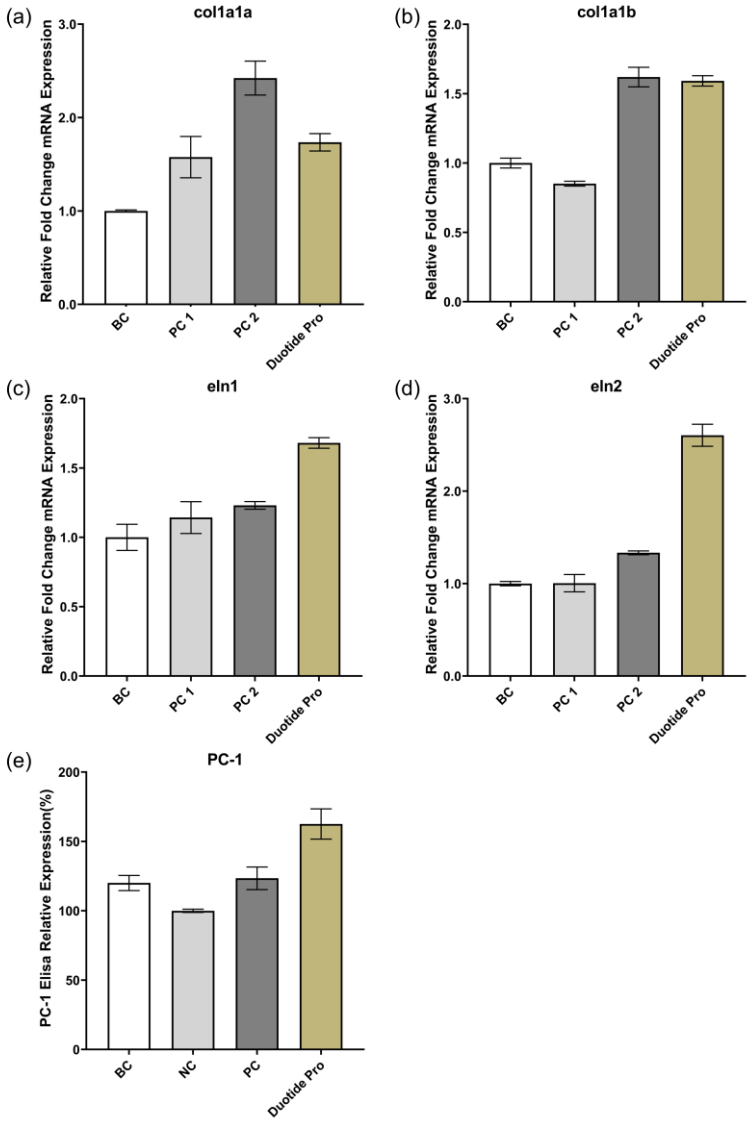

Figure 5. Testing of Duotide Pro for anti-wrinkle, firming and anti-aging effects. (a) Col1a1a gene expression; (b): Col1a1b gene expression; (c): Eln1 gene expression; (d): Eln2 gene expression; BC: Blank control; PC 1: 0.01% L-Carnosine; PC 2: 0.03% L-Carnosine; 2% Duotide Pro (0.0002% Palmitoyl Hexapeptide-12 and 0.001% Nonapeptide-1); (e): PC-1 secretion levels; BC: Blank control; NC: Negative control; PC: 100μg/ml VC+7μg/ml VE; 1% Duotide Pro (0.0001% Palmitoyl Hexapeptide-12 and 0.0005% Nonapeptide-1)

Table 5. The encapsulation efficiency of Duotide Pro

Batch number	EE (%)	
	Baseline	Month 6
2403	99.03	98.22
2408	98.31	97.75
2411	98.77	98.13

4. Discussion

A novel nanoliposome of GHK-Cu@GS-LP was prepared for enhancing transdermal absorption and anti-aging effectiveness. Compared to GHK-Cu@LP, GHK-Cu@GS-LP has smaller particle size because the interaction between GS and GHK-Cu made liposomes more concentrated and stable. This study delved into the interactions between GHK-Cu and GS through various spectroscopic methods. The result of FTIR showed the complex formation of GHK-Cu-GS by C=O peak appearance in its spectrum. Resonance Light Scattering (RLS) experiments indicated that there is an interaction between GS and GHK-Cu to form a stable composite, and the particle size of the composite is relatively large. Thermodynamic parameters (ΔH, ΔS, ΔG) suggested that hydrophobic interaction and hydrogen bond maintained the GHK-Cu-GS complex system. Synthesizing the above experimental data, it was proved that GS formed complexes with GHK-Cu, thereby altering the spatial conformation and physical properties of GHK-Cu.

Based on data of UPLC-QTOF-MS, the complexes of GHK-Cu-Rg1 and GHK-Cu-Rg2 were identified by UNIFI platform. The binding constants were calculated and indicated that the binding interactions between GHK-Cu and Rg1, Rg2 were particularly strong. Both Rg1 and Rg2 belong to the protopanaxatriol group of ginsenosides, suggesting that the molecular structure of protopanaxatriol ginsenosides is more conducive to form complex with GHK-Cu, compared to the protopanaxadiol group.

We developed co-delivered ginsenoside liposomes that effectively encapsulate both Palmitoyl Hexapeptide-12 (an insoluble ingredient) and Nonapeptide-1 (a water-soluble ingredient), resulting in high encapsulation efficiency to enhance their firming and anti-aging effects on the skin.

5. Conclusion

A novel nanoliposome of GHK-Cu@GS-LP was prepared and characterized using TEM and particle size analyzer in this study. GS was proved to have effect on making concentrated and stable liposomes, relating to the GHK-Cu-GS complex formation. The mechanism of complex formation was explored using multi-spectroscopic methods and UPLC-QTOF-MS coupled with UNIFI platform. The results of this study offer potential benefits for the cosmetic industry by using GS to enhance transdermal absorption and anti-aging effects of GHK-Cu containing products. Ginsenoside liposomes can encapsulate both water-soluble and insoluble active ingredients to enhance their anti-aging effects on the skin.

Acknowledgments

This work was supported by Jilin Provincial Natural Science Foundation [Grant no. YDZJ202501ZYTS578].

Conflict of Interest Statement

The authors declare no conflict of interest.

References

[1] LIU T, HU L, LU B, et al. A novel delivery vehicle for copper peptides [J]. New Journal of Chemistry, 2022, 47(1): 75-83.

[2] DYMEK M, OLECHOWSKA K, HAC-WYDRO K, et al. Liposomes as Carriers of GHK-Cu Tripeptide for Cosmetic Application [J]. Pharmaceutics, 2023, 15(10): 2485.

[3] HUR G-H, HAN S-C, RYU A R, et al. Effect of oligoarginine conjugation on the antiwrinkle activity and transdermal delivery of GHK peptide [J]. Journal of Peptide Science, 2020, 26(2): e3234.

[4] WANG Y, LIN J, CHENG J, et al. Rigid-flexible nanocarriers loaded with active peptides for antioxidant and anti-inflammatory applications in skin [J]. Colloids and Surfaces B-Biointerfaces, 2024, 236(4-6):113772.

[5] LIU L, ZHU X M, WANG Q J, et al. Enzymatic preparation of 20(S, R)-protopanaxadiol by transformation of 20(S, R)-Rg3 from black ginseng [J]. Phytochemistry, 2010, 71(13): 1514-20.

[6] LIN Y-P, ZHANG M-P, WANG K-Y, et al. Research achievements on ginsenosides biosynthesis from Panax ginseng [J]. Zhongguo Zhong Yao Za Zhi, 2016, 41(23): 4292-302.

[7] WANG H, ZHENG Y, SUN Q, et al. Ginsenosides emerging as both bifunctional drugs and nanocarriers for enhanced antitumor therapies [J]. Journal of Nanobiotechnology, 2021, 19(1): 322.

[8] SELVARAJ K, YOO B-K. Curcumin-Loaded Nanostructured Lipid Carrier Modified with Partially Hydrolyzed Ginsenoside [J]. Aaps Pharmscitech, 2019, 20(6): 252.

[9] HONG C, WANG D, LIANG J, et al. Novel ginsenoside-based multifunctional liposomal delivery system for combination therapy of gastric cancer [J]. Theranostics, 2019, 9(15): 4437-49.

[10] WANG J, ZHU H, LIU J H, et al. The effect of heparan sulfate on promoting amyloid fibril formation by β-casein and their binding research with multi-spectroscopic approaches. Journal of Photochemistry & Photobiology, B: Biology, 2020, 202, 111671.